2012

# The effects of annealing temperature on the in-field Jc and surface pinning in silicone oil doped MgB2 bulks and wires

M S. Hossain
*University of Wollongong*, shahriar@uow.edu.au

A Motaman
*University of Wollongong*, am107@uowmail.edu.au

O Cicek
*Ankara University*

H Agil
*Ankara University*

E Ertekin
*Ankara University*

*See next page for additional authors*

# The effects of annealing temperature on the in-field Jc and surface pinning in silicone oil doped MgB2 bulks and wires




## Publication Details

Hossain, M. S., Motaman, A., Cicek, O., Agil, H., Ertekin, E., Gencer, A., Wang, X. L. & Dou, S. X. (2012). The effects of annealing temperature on the in-field Jc and surface pinning in silicone oil doped MgB2 bulks and wires. Cryogenics, 52 (12), 755-759.



## Authors

M S. Hossain, A Motaman, O Cicek, H Agil, E Ertekin, A Gencer, Xiaolin Wang, and S X. Dou

# The Effects of Annealing Temperature on the in-field $J_c$ and Surface Pinning in Silicone Oil Doped $MgB_2$ Bulks and Wires

M. S. A. Hossain, A. Motaman, Ö. Çiçek, H. Ağıl, E.Ertekin, A. Gencer, , X. L.Wang, S. X. Dou

***Abstract*— The effects of sintering temperature on the lattice parameters, full width at half maximum (FWHM), strain, critical temperature ($T_c$), critical current density ($J_c$), irreversibility field ($H_{irr}$), upper critical field ($H_{c2}$), and resistivity (ρ) of 10 wt % silicone oil doped $MgB_2$ bulk and wire samples are investigated in state of the art by this article. The a-lattice parameter of the silicone oil doped samples which were sintered at different temperatures was drastically reduced from 3.0864 Å to 3.0745 Å, compared to the un-doped samples, which indicates the substitution of the carbon (C) into the boron sites. It was found that sintered samples at the low temperature of 600 ºC shows more enhancement in lattice distortion, more C-substitution, lower $T_c$, larger lattice strain, higher impurity scattering, and much more enhancement in both $J_c$ and $H_{c2}$, compared to those sintered samples at high temperatures. The flux pinning mechanism has been analyzed based on the extended normalized pinning force density $f_p = F_p/F_{p,max}$ scaled with $b = B/B_{max}$. Results show that surface pinning is the dominant pinning mechanism for the doped sample sintered at the low temperature of 600 ºC, while point pinning is dominant for the un-doped sample. The $MgB_2$ wire was also fabricated by using of this cheap doping and found that both $J_c$ and n-factor increased which proves this silicone oil doping can be a good candidate for industrial application.**

***Index Terms*—**

## I. INTRODUCTION

$MgB_2$ superconductor is a promising material for power applications, because of its high critical temperature ($T_c$) than Nb-Ti and $Nb_3Sn$ and a larger superconducting coherence length than the high temperature superconductors (HTS) [1]. $MgB_2$ is classified in two-gap superconductor, and it shows less weak-link and anisotropic effects [2, 3] compared to the HTS compounds. Due to the higher $T_c$ of 39 K and the lower fabrication cost, $MgB_2$ has been regarded as a promising candidate for practical applications, such as a cryogen-free magnetic resonance imaging (MRI) magnet which can operate at temperatures above 20 K [4]. Unfortunately, due to 8weak flux pinning, the critical current density ($J_c$) of un-doped $MgB_2$ drops quickly with increasing magnetic field at high temperatures. A significant enhancement in the $J_c$ and flux pinning in $MgB_2$ has already been achieved through chemical doping, especially when the dopants are on the nanoscale. For example, additions of nano-SiC [5-7], nano-Si [9], nano-C powders [10, 11], carbon nano-tubes (CNTs) [12], and carbohydrates (CH) [13] have all been found to be very effective in improving the field dependence of $J_c$ in $MgB_2$. However, all these chemicals are solid materials, which can cause resulted $MgB_2$ to have an agglomeration problem when they are blended together and this phenomenon leads to further limitation on improvements of the $MgB_2$ performance. Wang et al. reported that by adding a liquid additive, silicone oil, into the $MgB_2$, the $J_c$-$H$ properties can be significantly enhanced [14]. The advantage of the liquid silicone oil is that the mixing with Mg and B of either Si or C released from the decomposition of silicone oil takes place on the atomic scale and is more homogeneous than when solid nano powders are used. This homogeneity of mixing is very crucial in determination of the flux pinning ability for $MgB_2$ made by the *in-situ* reaction method. It was found that $MgB_2$ doped with 10 wt% silicone oil exhibits the largest $J_c$ in-field enhancement among a variety of samples sintered at the fixed temperature of 780 $^oC$ [14]. However, heat-treatment effects on the flux pinning performance have not yet been reported for silicone oil-doped $MgB_2$. In this work, we report a systematic study of the sintering temperature effect on the $MgB_2$ lattice parameters, C substitution levels, $T_c$, $J_c$, upper critical field ($H_{c2}$), and irreversibility field ($H_{irr}$) in 10 wt% silicone oil doped $MgB_2$ bulk samples as well as detailed study on the transport $J_c$ in 10 wt% silicon oil doped $MgB_2$ monofilamentary wire. It was figured out that low sintering temperatures can result in a large enhancement of the mangent and transport $J_c$ in-field performance in the silicone oil doped $MgB_2$. The possible flux pinning mechanism will also be discussed.

## II. EXPERIMENTAL

Amorphous boron (B) powders, Mg powders, and commercial high temperature silicone oil from Sigma Aldrich have been used as starting materials for this work. B and Mg powders in chemical stoichiometry were thoroughly mixed

Manuscript received October 9, 2001. (Write the date on which you submitted your paper for review.) This work was supported by funding from the Australian Research Council (ARC) under Linkage and ARC International Linkage projects and is partially supported by the Global Partnership Program through the Ministry os Science and Technology in Korea.

M. S. A. Hossain, A. Motaman, X. L. Wang and S. X. Dou are with the Institute for Superconducting and Electronic Materials, University of Wollongong, Innovation Campus, North Wollongong, NSW 2519, Australia (e-mail: Shahriar.Hossain@physics.unige.ch).

Ö. Çiçek, H. Ağıl, E. Ertekin and A. Gencer are with Ankara University, Faculty of Science, Department of Physics, Tandoğan 06100, Ankara, Turkey.

with diluted silicone oil. The amount of silicone oil added was 10 wt %. Pellets 13 mm in diameter and 2 mm in thickness were made under uniaxial pressure. Three samples were then sealed in an iron tube and sintered in-situ in a tube furnace at 600 °C for 4 hrs, and for 780 and 900 °C for 30 min, respectively. A high purity argon gas flow was maintained throughout the *in-situ* sintering process to avoid oxidation. Three un-doped $MgB_2$ samples (650, 800 and 900 °C for 30 min) were also prepared under the same conditions to serve as reference samples. The information from X-ray diffraction (XRD) on the crystal structures, such as the lattice parameters and the lattice strain, was refined by using the Rietveld refinement method. $T_c$ was defined as the onset temperature at which the diamagnetic property was observed. The resistivity and magnetization were measured at 5 and 20 K using a Physical Properties Measurement System (PPMS, Quantum Design) in magnetic fields up to 8.5 T. The magnetic $J_c$ was derived from the width of the magnetization loop using Bean's model. The $H_{c2}$ and $H_{irr}$ for all the samples were defined as $H_{c2} = 0.9R(T_c)$ and $H_{irr} = 0.1R(T_c)$ from the resistance ($R$) versus temperature ($T$ ) curve. For wire sample; 10 wt% silicon oil doped $MgB_2$ wire and one $MgB_2$ pure wire as a reference with 37% filling factor for both pure and doped wires were fabricated based on the powder in tube process with iron as an outer sheath. All manufactured wires were then covered by zirconium foil and sintered at 650 and $900^0$c in Ar atmosphere. The transport $J_c$ was measured at 4.2 and 20 k by using the 400 A power supply and four probes method with a criterion of $1\mu Vcm^{-1}$.

## III. RESULTS AND DISCUSSIONS

Fig. 1 shows the XRD patterns of all the samples produced at different sintering temperatures. It can be observed that both the un-doped and the silicone oil doped $MgB_2$ samples sintered within the range of 600-900 $^oC$ contain well developed $MgB_2$ phase with a small amount of MgO. Silicone oil doped $MgB_2$ sintered at 600 $^oC$ for 4 hrs clearly shows peaks from the $Mg_2Si$ phase. However, the amount of $Mg_2Si$ phase was significantly reduced for the samples sintered at higher temperatures, and it almost disappeared for samples sintered at 900 $^oC$. The decomposition mechanism of commercial silicone oil has been well described in our previous report [14].

Table.1 shows the *a*-axis lattice parameter as a function of sintering temperature for both the un-doped and the silicone oil doped samples. It can be seen that the *a*-axis lattice parameter decreases from 3.086 to 3.076 Å for the pure and 10 wt % silicone oil doped samples, respectively. The *c*-axis lattice parameter is almost constant (inset) for both un-doped and doped samples sintered at different temperatures. The significant reduction in the *a*-axis lattice parameter indicates that carbon substitutes into the B sites in the crystal lattice.

Table.1 also shows the calculated *c/a* ratios of un-doped samples sintered at different temperatures. The silicone oil doped $MgB_2$ also shows a similar trend, suggesting that C substitution for B occurred in the silicone oil added samples. According to the method proposed by Avdeev *et al.* [15], the level of C substitution, *x*, in Mg $(B_{1-x}C_x)_2$, can be easily estimated using the formula $x = 7.5\times\Delta(c/a)$, where $\Delta(c/a)$ is the change in *c/a* when compared to an un-doped sample. We found that the actual amount of C ($x$) in the silicone doped samples increased from 0.004 to 0.023 as the sintering temperature increased from 600 to 900 $^oC$, as shown in table. 1. This result indicates that C substitution can take place even at the low sintering temperature of 600 $^oC$. This is one of the advantages of using the silicone oil as a C source, since low temperature heat-treatment processing can introduce strong grain boundary pinning, as well as C substitution effects at the same time.

The lattice strain *vs.* sintering temperature for both silicone oil doped and un-doped samples is shown in table.1. The strain decreases with increasing sintering temperature. This is probably related to the C-substitution and to defects within the grains, as mentioned above. in another word, the improvement of crystallinity due to grain growth may reduce defects within grains for samples sintered at high temperatures. As a result, there is a strong correlation between strain and $T_c$. The sample sintered at 600 $^oC$ shows a relatively higher strain value, ~0.57%, than other samples. This also indicates that various trapped defects within $MgB_2$ grains might act as flux pinning centers.

Among the various XRD peaks, the full width at half maximum (FWHM) of the (110) peak is related to the *in-plane* crystallinity. According to Williamson-Hall, the strain and grain size can both affect the FWHM value [16]. So far as strain is concerned, there are actually two types of strain in samples, micro-strain and macro-strain. The micro-strain varies from one grain to another one in the microscopic scale, resulting in non-uniformity, which produces peak broadening. On the other hand, macro-strain is uniform, and its uniform effects can produce peak shifting. The former is due to the contribution of defects inside grains as well as the $MgB_2$ grain size which varies from small grain to large grain due to sintering temperature, and the latter is due to the substitution of elements such as C into B sites [17]. Analysis of the FWHM can provide considerable information on the crystallite size and on the micro-strain in the lattice that is presented in the specimen. Table.1 also shows the $T_c$ and the FWHM of the (110) peak *vs.* sintering temperature. The FWHM decreases as the sintering temperature increases in both un-doped and silicone oil doped samples. According to Scherrer's formula, the FWHM value is inversely proportional to grain size. The values of the FWHM for the doped samples are greater than for the un-doped samples. This means that the grain sizes in the doped samples are smaller than in the un-doped samples, regardless of sintering temperature.

On the other hand, $T_c$ shows an opposite trend to the FWHM, as shown in table.1. The increase in $T_c$ indicates better crystallinity or less crystal defects in the samples sintered at high temperatures than those sintered at low temperatures. Improvement on crystallinity should also be accompanied by better grain connectivity of the $MgB_2$ grains. On the other hand, the significant suppression of crystallinity for silicone oil doped $MgB_2$ sintered at 600 $^oC$ likely originates from disorder in the crystal lattice due to the C substitution.

Table.1 illustrates the measured ρ values, RRR ($\rho_{300\ K}/\ \rho_{40K}$), and active cross-sectional area fraction ($A_f$) for silicone oil doped $MgB_2$ samples with different sintering temperatures.

it was observed that ρ at 300 K decreases with increasing sintering temperature. This is related to the better crystallinity of $MgB_2$ phase that arises from additional grain growth, as mentioned above. Specifically, the relatively lower ρ near 300 K may be related to higher sample density and better inter-granular connectivity. On the other hand, the resistivity values near the transition temperatures are due to the intra-granular defects, since the phonon contribution to the electron scattering decreases when the temperature decreases. The defects inside grains may also affect the ρ at 40 K [18]. These observations can be further supported by the Δρ and RRR behavior. It is well known that relatively high values of the RRR indicate good quality of samples. The connection factor, $A_f$, was also evaluated using the Rowell analysis [18]. As shown in the Table 1, the values of $A_f$ increase from 0.137 to 0.327 as the sintering temperature increases from 600 to 900 ºC.

Fig. 2 shows the magnetic $J_c$ of the un-doped and the silicone oil added $MgB_2$ samples as a function of sintering temperature. It can be seen that the $J_c$ values of the un-doped sample sintered at 650 ºC and 900 ºC for 30 minutes are higher than those of the silicone oil doped samples in the low magnetic field region at both 5 and 20 K. As field increased, the $J_c$ values at 20 K for the doped samples sintered at 900 ºC were much higher than those for the un-doped samples at fields greater than 3 T. This is the indication of flux pinning strength enhancement in the silicone oil doped samples. At the same time, the $J_c$ values of the doped samples are strongly dependent on the sintering temperature. The $J_c$ values at 5 K for the doped samples sintered at 600 ºC are higher than for those sintered at 900 ºC up to a field of 8.7 T. However, at 20 K, the sample sintered at 900 ºC shows higher $J_c$ values than the 600 ºC sample for fields above 1 T. The $J_c$ values of the samples sintered at 600 ºC and 900 ºC were approximately 1.2 $\times 10^4$ A/cm$^2$ at 5 K and 8 T. At 5 K and 5T the $J_c$ value for the 600 ºC sample was $9 \times 10^4$ A/cm$^2$, but $5 \times 10^4$ A/cm$^2$ for the 900 ºC sample. These $J_c$ values for the silicone oil doped $MgB_2$ are as high as the best $J_c$ values obtained in $MgB_2$ samples doped with solid nano-SiC. This indicates that the liquid additive, silicone oil, is a cheap and convenient alternative dopant to replace solid nano-SiC powders.

The temperature dependency of $H_{c2}$ and $H_{irr}$ for the un-doped and silicone oil added $MgB_2$ samples is shown in Fig. 3. The values of $dH_{c2}/dT$ and $dH_{irr}/dT$ for the silicone oil added $MgB_2$ samples increase more quickly than un-doped $MgB_2$ samples. Furthermore, these values are almost independent of sintering temperature. It is well known that an enhancement of $H_{c2}$ indicates that both intra-band and inter-band scattering are enhanced and it is due to C substitution into the B sites. It should be noted that the sample sintered at 600 ºC shows almost the same $H_{irr}$ value as that sintered at 900 ºC, suggesting that a low sintering temperature is more effective in enhancing the flux pinning, due to active C substitution and a high density of grain boundaries. However, using high resolution transmission electron microscopy is needed for further study on the grain sizes and crystal defects. The presence of $Mg_2Si$ impurity phase is also responsible for the peak broadening, as the $Mg_2Si$ is believed to act as a grain refiner in silicone oil doped $MgB_2$ at lower sintering temperatures [19]. Therefore, the enhanced flux pinning, $H_{c2}$, $H_{irr}$, and $J_c$-$H$ observed in our silicone oil added $MgB_2$ that was sintered at 600 ºC are likely due to the C-doping effect and inclusions of $Mg_2Si$.

Plots of normalized pinning force density $f_p = F_p/F_{p,max}$ against reduced field are shown in Fig.7. The equation $f_p(b) = Ab^p(1-b)^q$ is usually employed as a single pinning function, where $p$ and $q$ are parameters describing the particular type of pinning, and $b$ is the reduced field, with $b = B/B_{irr}$ [20]. In this model, $p = 1/2$ and $q = 2$ describe surface pinning, while $p = 1$ and $q = 2$ describes point pinning, as predicted by Kramer [21]. The best fit of the curves (solid curves in Fig. 4(a)) are obtained with $p = 0.8$ - $1.2$ and $q = 2.9$ - $3.4$ for all samples at T = 20 K. These two values obtained do not allow us to infer the real dominant pinning mechanism from this scaling behavior.

For obtaining a deeper insight into the pinning mechanism, the extended normalized pinning force density $f_p = F_p/F_{p,max}$, plotted against $b = B/B_{max}$ instead of $b = B/B_{irr}$, was examined, where $B_{max}$ is the magnetic field at the maximum of $F_p$ [22]. The scaling of $f_p$–$b$ is often analyzed in terms of normal point pinning, $f(b) = (9/4)b(1-b/3)^2$ and surface pinning, $f(b) = (25/16)b^{0.5}(1-b/5)^2$, which has been inferred by Higuchi *et al*. [22]. The fitting results are shown by the solid curves in Fig. 4(b). In low magnetic fields, the experimental data are in good agreement with the point pinning mechanism for all samples. At normalized magnetic fields higher than $b_{max}$, flux pinning is dominated by surface pinning for the doped sample sintered at 600 ºC, while point pinning is dominant for the un-doped sample. For the doped sample sintered at 900 ºC, the experimental data are located between the theoretical curves for surface pinning and point pinning. Therefore, flux pinning is determined by both point pinning and surface pinning for this sample. These results are in good agreement with the fact that the grain sizes of the doped $MgB_2$ sintered at 600 ºC are much smaller than for the sample sintered at 900 ºC. This means that the grain boundary density and its contribution to flux pinning are dominant in the samples sintered at low temperature.

Fig.5 shows the transport $J_c$ of doped and un-doped $MgB_2$ wire at different high applied fields. It has to be noted that the transport $J_c$ measurements cannot be done at low field due to the limitation of current flow (250 A) into the probe, therefore high field results can be seen in Fig.5. Doping of silicone oil causes a gradual shift of the curve $J_c$ versus $B$ towards higher values. At 600 ºC, the value of $B(10^4)$ [where the field at which $J_c$ reaches to $10^4$ A/cm$^2$]was enhanced from 7.5 to 9.1 T, or by 1.6 T. The transport $J_c$ values of the sintered sample at 600ºc is higher than sintered sample at 900ºc because of defects originated from higher strain and carbon substitution at low sintering temperature as evidenced by table 1, therefore, low sintering temperature is more beneficial for grain boundary pinning due to an increase in density of grain boundaries.

In view of MRI or low field NMR applications, the exponential $n$ factor plays an important role. It is known that at 4.2 K and low fields, $n$ of $MgB_2$ wires can reach very high values. However, the strong decrease of $n$ with field is a limiting factor when envisaging applications at higher fields. As shown in Fig. 6, the silicone oil doped wire leads to a

considerable increase of the *n* factor. The data set is not complete yet, but it can be seen that the increase of *n* after doping at 650 ºC is around 33%. For example, the field at which *n* takes the value 30 is higher in silicone doped wires, the average enhancement being estimated to ~ 1T at 20K and ~ 2 T at 4.2 K. This argument is of industrial importance. Although *n* is an empirical factor which depends on a variety of effects which are not all well defined, it reflects in a certain way the homogeneity of a filament. The present enhancement of *n* can thus be interpreted as an improved homogeneity of the silicone oil doped filament (this is also confirmed by the analysis of the electrical resistivity presented in table 1).

In summary, we have found that the sintering temperature has a significant effect on the flux pinning enhancement in $MgB_2$ doped with a liquid additive, silicone oil. The low sintering temperature of 600 ºC can lead to a reduction of the lattice parameters and RRR values, resulting in a significant enhancement of $H_{c2}$, $H_{irr}$, and both magnetic and transport $J_c$-$H$. Surface pinning is the dominant pinning mechanism for the doped sample sintered at 600 ºC, while point pinning is dominant for the un-doped sample. Enhancement of n-value shows better homogeneity in sample sintered at 600' C.

## REFERENCES


[1] J. Nagamatsu, N. Nakagawa, T. Muranaka, Y. Zenitani and J. Akimitsu, 2001 *Nature* **410** 63.

[2] D. C. Larbalestier, L. D. Cooley,M. O. Rikel, A. A. Polyanskii, J. Jiang, S. Patnaik, X. Y. Cai, D. M. Feldmann, A. Gurevich, A. A. Squitieri, M. T. Naus, C. B. Eom, E. E. Hellstrom, R. J. Cava, K. A. Regan, N. Rogado, M. A. Hayward, T. He, J. S. Slusky, P. Khalifah, K. Inumaru and M. Haas, 2001 Nature 410 186.

[3] M. Kambara, B. N. Hari, E. S. Sadki, J. R. Cooper, H. Minami, D. A. Cardwell, A. M. Campbell and I. H. Inoue, 2001 *Supercond. Sci. Technol.* 14 L5-7.

[4] Y. Iwasa, D. C. Larbalestier, M. Okada, R. Penco, M. D. Sumption and X. Xi, 2006 *IEEE Tans. Appl. Supercond.* 16 1457.

[5] S. X. Dou, S. Soltanian, J. Horvat, X. L. Wang, S. H. Zhou, M. Ionescu, H. K. Liu, P. Munroe and M. Tomsic, 2002 *Appl. Phys Lett.* 81 3419.

[6] H. Kumakura, H. Kitaguchi, A. Matsumoto and H. Hatakeyama, 2004 *Appl. Phys. Lett.* 84 3669.

[7] M. D. Sumption, M. Bhatia, M. Rindfleisch, M. Tomsic, S. Soltanian, S. X. Dou and E. W. Collings, *Appl. Phys. Lett.* 86 092507.

[8] X. L. Wang, S. H. Zhou, M. J. Qin, P. R. Munroe, S. Soltanian, H. K. Liu and S. X. Dou, 2003 *Physica C* 385 461.

[9] X. L. Wang, S. Soltanian, M. James, M. J. Qin, J. Horvat, Q. W. Yao, H. K. Liu and S. X. Dou, 2004 *Physica C* 408–410 63.

[10] R. H. T. Wilke, S. L. Bud'ko, P. C. Canfield, D. K. Finnemore, R. J. Suplinskas and S. T. Hannahs, 2004 *Phys. Rev. Lett.* 92 217003.

[11] W. K. Yeoh, J. H. Kim, J. Horvat, X. Xu, M. J. Qin, S. X. Dou, C. H. Jiang, T. Nakane, H. Kumakura and P. Munroe, 2006 *Supercond. Sci. Technol.* 19 596.

[12] J. H. Kim, W. K. Yeoh, M. J. Qin, X. Xu, S. X. Dou, P. Munroe, H. Kumakura, T. Nakane and C. H. Jiang, 2006 *Appl. Phys. Lett.* 89 122510.

[13] J. H. Kim, S. H. Zhou, M. S. A. Hossain, A. V. Pan and S. X. Dou, 2006 *Appl. Phys. Lett.* 89 142505.

[14] X. L. Wang, Z. X. Cheng and S. X. Dou, 2007 *Appl. Phys. Lett.* 90 042501.

[15] M. Avdeev, J. D. Jorgensen, R. A. Ribeiro, S. L. Bud'ko and P. C. Canfield, 2003 *Physica C* 387 301.

[16] G. K. Williamson and W. H. Hall, 1953 *Acta Metall.* 1 22.

[17] S. M. Kazakov, R. Puzniak, K. Rogacki, A. V. Mironov, N. D. Zhigadlo, J. Jun, Ch Soltmann, B. Batlogg and J. Karpinski, 2005 *Phys. Rev. B* 71 024533.

[18] J. M. Rowell, 2003 *Supercond. Sci. Technol.* 16 R17.

[19] S. Soltanian, X. L. Wang, J. Horvat, S. X. Dou, M. D. Sumption, M. Bhatia, E. W. Collings, P. Munroe and M. Tomsic, 2005 *Supercond. Sci.Technol.* 18 658.

[20] D. Dew-Hughes, 1974 *Phil. Mag.* 30 293.

[21] E. J. Kramer, 1974 *J. Appl. Phys.* 44 1360.

[22] T. Higuchi, S. I. Yoo and M. Murakami, 1999 *Phys. Rev. B* 59 1514.

**Table caption:**

Table 1. The resistivity at 40 K and 300 K, $\Delta\rho = \rho_{300\ K} - \rho_{40\ K}$, the RRR, the connectivity factor $A_f$ of 10 wt % silicone oil doped $MgB_2$ as well as all crystallography data resulting from different sintering temperatures.

**Figure captions:**

Fig.1. XRD patterns for the un-doped $MgB_2$ sintered at 650 ºC and 900 ºC and the silicone oil doped $MgB_2$ samples sintered at 600 and 900 ºC.

Fig.2. The magnetic field dependence of $J_c$ at 5 and 20 K for un-doped $MgB_2$ sintered at 650 ºC and 900 ºC and silicone oil doped $MgB_2$ sintered at 600 and 900 ºC .

Fig.3. $H_{c2}$ and $H_{irr}$ *vs.* normalized temperature for un-doped and silicone oil doped $MgB_2$.

Fig.4. Magnetic field dependence of the reduced pinning force $f(b)$ at 20 K: (a) $b = B/B_{irr}$ and (b) $b = B/B_{max}$ for un-doped $MgB_2$ sintered at 650 ºC and silicone oil doped $MgB_2$ samples sintered at 600 and 900 ºC. Solid curves are fittings to models.

Fig. 5. The transport critical current density at 4.2 and 20 K as a function of sintering temperature. Un-doped $MgB_2$ wire is also shown as a reference.

Fig.6. The n-value at 4.2 and 20 K as a function of sintering temperature.

**Table 1.**

| **Samples** | **Sintering conditions** | **$\rho_{300\ K}$ (μΩcm)** | **$\rho_{40\ K}$ (μΩcm)** | **Δρ (μΩ.cm)** | **RRR** | **$A_f$** | **a(ºA)** | **c/a** | **Strain %** | **FWHM** | **$T_c$** |
|---|---|---|---|---|---|---|---|---|---|---|---|
| $MgB_2$ + 10% Silicone oil | 600ºC x 4 hour | 150.34 | 97.31 | 53.03 | 1.54 | 0.137 | 3.078 | 1.1434 | 0.575 | 0.676 | 35.2 |
| $MgB_2$ + 10% Silicone oil | 780ºC x 30min | 128.56 | 87.67 | 40.89 | 1.47 | 0.178 | 3.075 | 1.1465 | 0.475 | 0.6 | 36.2 |
| $MgB_2$ + 10% Silicone oil | 900ºC x 30min | 65.85 | 43.56 | 22.29 | 1.51 | 0.327 | 3.077 | 1.1444 | 0.44 | 0.55 | 36.35 |
| $MgB_2$ un-doped | 650ºC x 30min | 77.3 | 41.8 | 35.5 | 1.85 | 0.211 | 3.086 | 1.143 | 0.56 | 0.56 | 36.67 |
| $MgB_2$ un-doped | 800ºC x 30min | 56.4 | 27.3 | 29.1 | 2.06 | 0.252 | 3.085 | 1.1432 | 0.375 | 0.475 | 37.5 |
| $MgB_2$ un-doped | 900ºC x 30min | 53.4 | 24.8 | 28.6 | 2.46 | 0.261 | 3.084 | 1.1415 | 0.36 | 0.44 | 38.3 |

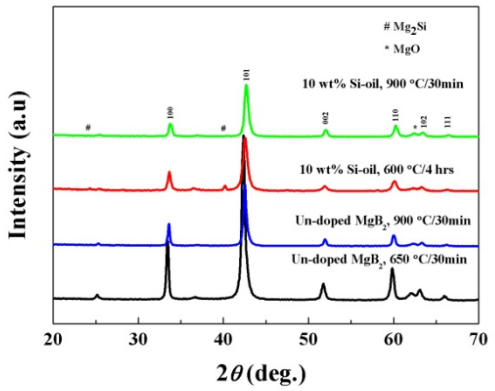


Fig. 1.

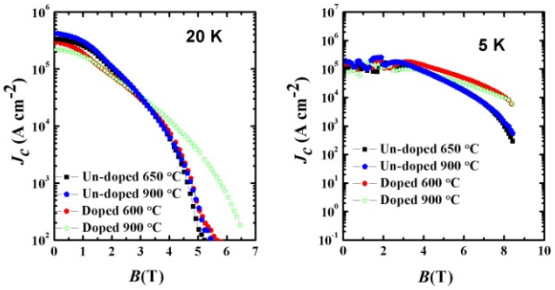


Fig. 2.

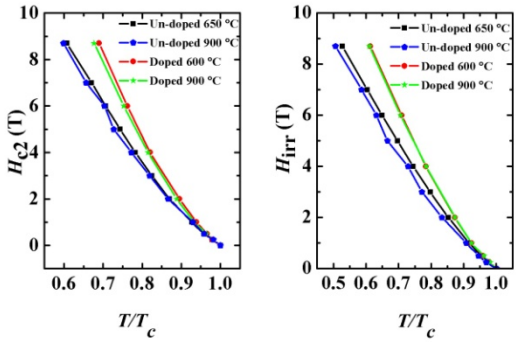


Fig. 3.

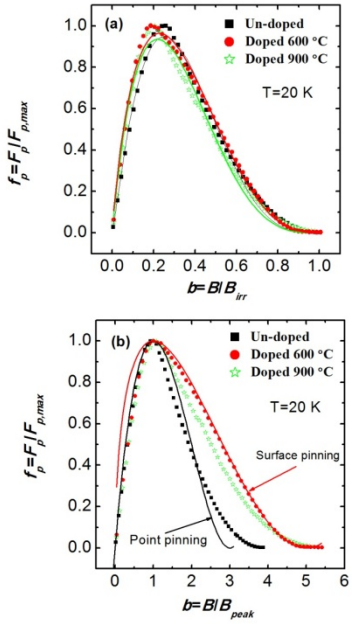


Fig. 4.

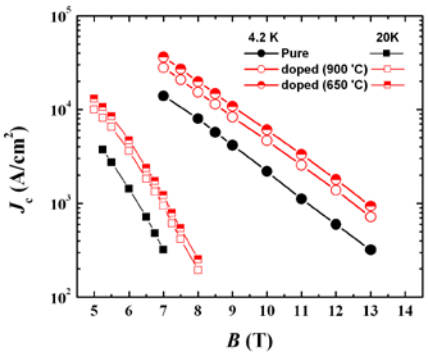


Fig. 5.

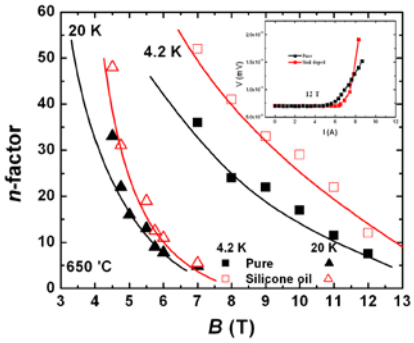


Fig. 6.